INT. J. NUM. METH. HEAT FLUID FLOW, VOL. 4, 207–227 (1994)

NUMERICAL INVESTIGATION OF THE COMBINED EFFECT OF SWIRLER AND PRIMARY JETS ON THE RECIRCULATION ZONE OF A CAN-TYPE COMBUSTOR BY MEANS OF AN ORTHOGONAL ARRAY TECHNIQUE

R. GOPINATH AND V. GANESAN

Department of Mechanical Engineering, Indian Institute of Technology, Madras-600036, India

ABSTRACT

An orthogonal array technique is used in the present work to investigate, numerically, the effects of the swirler and the primary jets on the characteristics of the recirculation zone of a can-type gas turbine combustor. The computer code used for this purpose is first validated with the available experimental data. The effects of change in the percentage flow rate through the swirler, the swirl number, the hub diameter of the swirler and the diameter of the primary injection holes (which influences the velocity of the jets) are estimated first. It is found that the flow rate through the swirler and the size of the primary injection hole have much more influence on the characteristics of the recirculation zone than the swirl number and the hub diameter of the swirler. But the earlier studies show that for a given flow rate through the swirler, the swirl number and swirler geometry have considerable influence on the characteristics of the recirculation zone in the absence of primary jets. Therefore it is inferred that there may be a critical point, based on the ratio of flow rate through the swirler to that of primary holes, beyond which the effects of swirl number and the swirler geometry dominate the effect of primary jets in determining the characteristics of the recirculation zone. This critical point is determined by gradually reducing the flow through the primary holes. It is found that, initially, the recirculation ratio (ratio of the mass of fluid recirculated to that sum of the mass flow rate through the swirler and through that of primary hole) reduces because of weakening of the primary jets but after the critical point it increases because of the swirler effect taking over the role of providing the recirculation. It is also observerd that the length of the recirculation zone increases as the strength of the primary jets reduces.

KEY WORDS Orthogonal arrays Recirculation Swirler primary jets Design of experiments

INTRODUCTION

Due to the complexity of the flow in a gas turbine combustor the approach usually adopted for experimental investigation, and also for numerical modelling, is to divide the real flow into a number of well-controlled component flows, each emphasizing only one or two aspects of the flow at a time. Some researchers have considered axisymmetric geometries without primary and dilution jets and focused their attention on the influence of swirl on the simulated primary zone flow structure[1–4]. On the other hand some researchers have studied only the dilution zone region and behaviour of rows of jets in a cross-flow in isolation.

The most comprehensive study to date, which takes into account all the aspects of a three-dimensional combustor flow viz., swirl, impinging jets, nozzle effects, is that of Koutmos and McGuirk [6–8]. The effect of variation of the flow split, between the swirler and the primary and dilution holes on the flow pattern in the primary zone of a water model of a can combustor,

0961–5539/94/030207–21$2.00

Received February 1993
Revised August 1993

was investigated both experientally and numerically. However, in this study, the velocity of the primary jet was kept for all the flow splits. Additionally, experiments were carried out for a very narrow range of swirl numbers i.e., from 0.75 to 0.85.

The scope of this work is to numerically investigate the effect of varying the primary jet injection velocity, the swirler geometry and swirl number (wider range −0.5 to 1.0) in addition to varying flow splits, on the recirculation zone characteristics. The novelty of this study is in the use of an orthoganal array technique (OAT) for deciding the combinations of the above factors for various trials and for analyzing the results. This technique is more advantageous than classical one-factor-at-a-time method of performing experiments since OAT can detect interactions between various parameters, thereby avoiding false optimum settings. Besides, it is possible, using this technique, to quantify the relative individual effects and interaction effects of the parameters towards the variation of the variable of interest.

DESCRIPTION AND VALIDATION OF THE NUMERICAL CODE

The code developed is a three-dimensional finite difference code based on the SIMPLE algorithm of Patankar and Spalding[9]. This predicts for turbulent recirculating flows the hydrodynamic variables viz., u, v, w, k, and ϵ, by solving the equation:

$$\frac{\partial(\rho\phi)}{\partial t} + \text{div}(\rho u\phi - \Gamma \text{ grad } \phi) = S$$

where ϕ is the dependent variable, Γ is the exchange coefficient and S denotes the source term. The values of Γ and S corresponding to ϕ is available in [10] and also in *Table 1*.

The predicted results of this code have been compared with the experimental results reported by Koutmos and McGuirk[6] for the model combustor geometry shown in *Figure 1*. The experimental model is made of perspex and consists of a hemispherical section attached to a central barrel of 74 mm internal diameter to which a circular to rectangular contraction nozzle is attached on the other end. This combustor is located concentrically in a tube of a larger internal diameter of 160 mm. Curved vane aerodynamic swirler is attached to the head. Six equispaced primary holes of 10 mm diameter are located 46 mm downstream of the swirler. At a distance of a further 80 mm downstream, twelve equispaced holes, also of 10 mm diameter, are located. Two constant head water tanks are provided – one supplying independently to the swirler and the other to the larger outer tube to provide an annular feed to both primary and dilution holes.

Figure 2 shows the radial variation of axial velocity (normalized with respect to bulk velocity), both predicted and measured, for six stations. The stations 'b' and 'c' lie in the primary zone. The axis of the primary hole is located at station 'd'. The stations 'g' and 'j' lie in the region between the rows of primary and secondary holes. The axis of the secondary hole is located at station '1'. *Figure 3* shows the axial variation of the centerline axial velocity.

It is clear that the trends are predicted quite well at all of the stations. Quantitatively, the velocities are underpredicted at the axis, the maximum being of the order of 25% at station 'c'. The agreement improves for all the stations, except '1', as we move away from the centerline. The discrepancy is more at the station '1' on account of its proximity to the contraction nozzle, the effect of which has not been considered during the numerical calculations due to its complex geometry.

The predicted radial and tangential velocities and turbulent kinetic energy has also been compared with that obtained from experiments and has been reported elsewhere[11,12]. The velocities show reasonably good quantitative as well as qualitative agreement but agreement of values of kinetic energy can be considered only qualitative.

The area having negative axial velocity, i.e. the recirculation zone is shown in *Figure 4*. The

Table I Values of Φ, β, Γ and S

No.	Equation	ϕ	β	Γ	S_ϕ
1.	Continuity	1	ρ	0	0
2.	x-Momentum	u	ρ	μ	$-\frac{\partial p}{\partial x}+\frac{\partial}{\partial x}\left(\mu\frac{\partial u}{\partial x}\right)+\frac{1}{r}\frac{\partial}{\partial r}\left(r\mu\frac{\partial v}{\partial x}\right)+\frac{1}{r}\frac{\partial}{\partial \theta}\left(\mu\frac{\partial w}{\partial x}\right)$
3.	r-Momentum	v	ρ	μ	$-\frac{\partial p}{\partial r}+\frac{\partial}{\partial x}\left(\mu\frac{\partial u}{\partial r}\right)+\frac{1}{r}\frac{\partial}{\partial r}\left(r\mu\frac{\partial v}{\partial r}\right)+\frac{1}{r}\frac{\partial}{\partial \theta}\left[\mu\left(\frac{\partial w}{\partial r}-\frac{w}{r}\right)\right]+\frac{\rho w^2}{r}-\frac{2\mu}{r}\left(\frac{\partial w}{r\partial \theta}+\frac{v}{r}\right)$
4.	θ-Momentum	w	ρ	μ	$-\frac{1}{r}\frac{\partial p}{\partial \theta}+\frac{\partial}{\partial x}\left(\frac{\mu\partial u}{r\partial \theta}\right)+\frac{1}{r}\frac{\partial}{\partial r}\left[\mu r\left(\frac{l\partial v}{r\partial \theta}-\frac{w}{r}\right)\right]-\frac{\rho v w}{r}+\frac{1}{r}\frac{\partial}{\partial \theta}\frac{\mu}{r}\left(\frac{\partial w}{\partial \theta}+2v\right)+\frac{\mu}{r}\left(\frac{\partial w}{\partial r}+\frac{\partial v}{r\partial \theta}-\frac{w}{r}\right)$
5.	Turbulence energy	k	ρ	$\frac{\mu_{eff}}{\sigma_{eff}}$	$G_k-C_\mu\varepsilon\rho$ $\quad C_\mu=0.09$
6.	Rate of energy dissipation	ε	ρ	$\frac{\mu_{eff}}{\sigma_{eff}}$	$(C_1G_k-C_2\rho\varepsilon)\cdot\varepsilon/k$ $\quad C_1=1.43$, $C_2=1.92$

$$G_k=\mu_t\left[2\left(\frac{\partial u}{\partial x}\right)^2+\left(\frac{\partial v}{\partial r}\right)^2+\left(\frac{\partial w}{r\partial \theta}+\frac{v}{r}\right)^2+\left(\frac{\partial w}{\partial x}+\frac{\partial u}{r\partial \theta}\right)^2+\left(\frac{\partial u}{\partial r}+\frac{\partial v}{\partial x}\right)^2+\left(\frac{\partial w}{\partial r}+\frac{\partial v}{r\partial \theta}-\frac{w}{r}\right)^2\right]$$

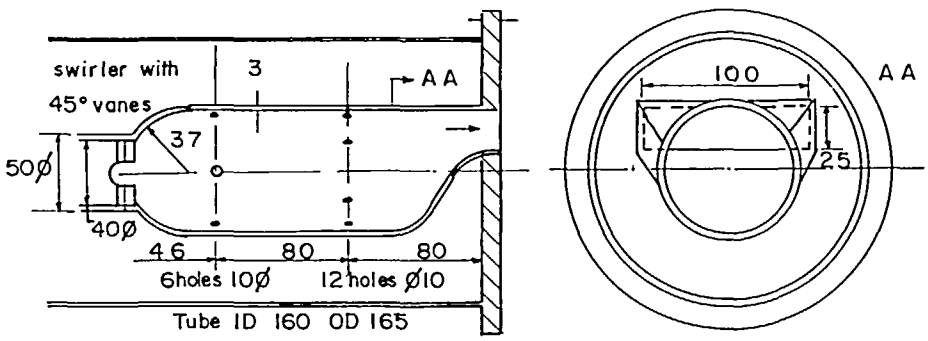

Figure 1 Geometry of the combustor

predicted and the actual recirculation zone is compared on the basis of its maximum length L, maximum thickness T and a parameter called recirculation ratio R, defined as

$$R=\dot{m}_r/(\dot{m}_{sw}+\dot{m}_{pr})$$

where $\dot{m}_{sw}$ is the mass flow rate through the swirler, $\dot{m}_{pr}$ is the mass flow rate through the primary air injection hole and $\dot{m}_r$ is the mass of the fluid recirculated in the primary zone which is found

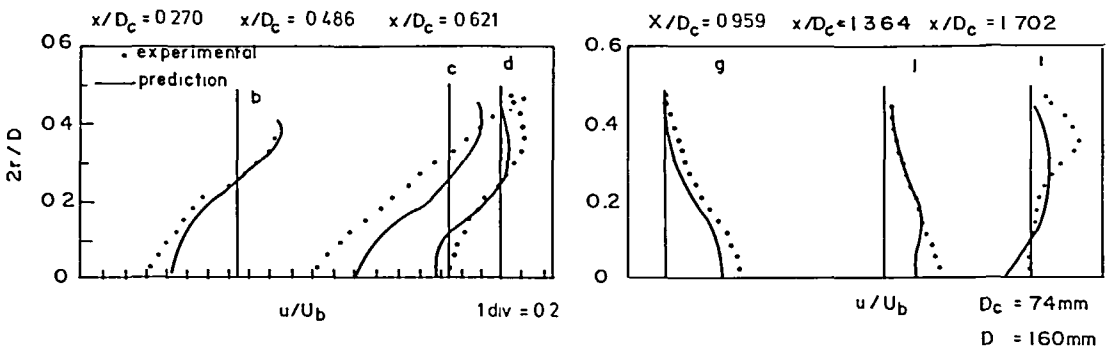

Figure 2 Variation of axial velocity with x/D_c

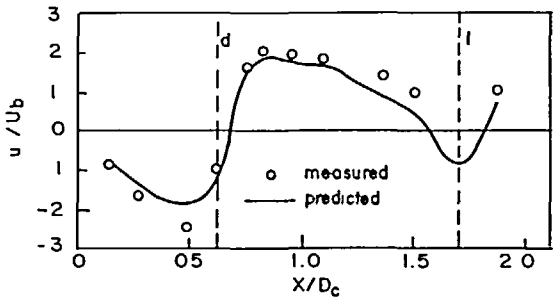

Figure 3 Centerline axial velocity

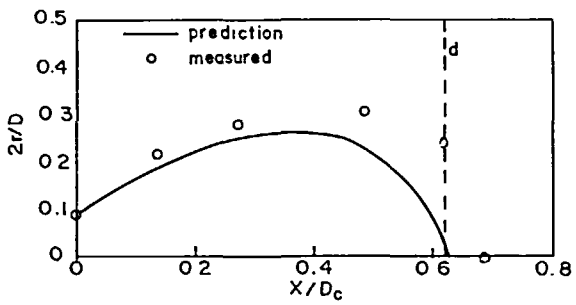

Figure 4 Recirculation zone

by integration of the negative part of the axial velocity profile at plane 'c' which is located at a distance of 36 mm from the inlet. This station has been chosen because of its proximity to the eye of the primary vortex[7].

Comparison of predicted and experimental values of R, L and T are shown in *Table 2*. We find that R is underpredicted by about 25%. L and T are also underpredicted by about 10% and 20%, respectively.

The results discussed above are for a swirler flow rate of 15% of the total flow. The general input assumptions for predicting the variables are viz., uniform axial velocity; linearly varying azimuthal (swirl) velocity based on the mass flow rate and swirl number; zero radial velocity

Table 2 Comparison of recirculation zone characteristics

	Experimental	Predicted
R	0.63	0.47
L (mm)	51	47
T (mm)	26	21

at the swirler; radial velocity at injection holes based on mass flow rate; cyclic boundary conditions for the 60° sector (since the geometry repeats itself for every 60°); boundary values of length scale proportional to port size; the zero gradient condition at the outlet. The results were found to be grid independent between the grid sizes 29 × 16 × 7 and 37 × 20 × 7. Better predictions would have been possible by using a more sophisticated turbulence model (the standard k–ε model is used here) or discretization technique (hybrid scheme is used here) and by taking into consideration the effect of the contraction nozzle. The primary aim here is to carry out numerical parametric studies, using OAT, to quantify the effects of the change in operating parameters, relative to that of original settings, on the recirculation zone characteristics. For such an exercise the existing agreement between predicted and measured values are reasonably good, especially for the recirculation zone which will be of primary importance in this work. Further, incorporation of more sophisticated turbulence model or discretization scheme will result in more computer storage and execution time. Since a number of trials based on OAT is the main aim of this paper the use of more complex models is not considered.

ORTHOGONAL ARRAY TECHNIQUE

The orthogonal array technique (OAT) is a type of design of experiments (DOE) technique. One can decide upon the combinations of operating parameters for various trials using this technique. DOE techniques are becoming popular for performing physical experiments on account of its several advantages over the classical one-factor-at-a-time strategy. It has also been successfully adapted for parametric studies using a numerical code[11,13]. Details regarding the advantages of DOE and OAT are available in References 13–15. Here, it is sufficient to say that using this technique one can detect interactions between several operating parameters thereby avoiding false optimum settings and, besides, one can also quantify the effects of varying operating parameters (called 'Factors' in DOE terminology) towards the variation of variables of interest.

According to the philosophy of DOE, full factorial experiments in which all possible combinations of factors considered are tried out, are the most efficient way to perform the experiments. One can estimate the main effects (individual effects) of all the factors considered and also all possible interactions between them by performing full factorial experiments. However, when the number of factors considered are large, performing a full factorial experiment may not be economical and so one should use fractional factorial experiments. In fractional factorial experiments, based upon previous experience, it is arbitrarily decided not to estimate the effect of certain interactions and, as a result, the number of trials required to be performed is reduced. For example, if there are five factors each having two possible values (called 'Level' in DOE terminology and denoted by 1 and 2) then to estimate the main effects and all possible interactions between them one should perform full factorial experiments which would require $2^5 = 32$ trials. On the other hand, if we choose to estimate the main effects and first order interactions (simultaneous influence of only two factors) only, then a half factorial experiment can be performed which would require only 16 trials. If only main effects are to be estimated, only a quarter factorial experiment, 8 trials, is required.

Orthogonal arrays are the means to design factorial and fractional factorial experiments. An

Table 3 L9 array

Experiment	Columns 1	2	3	4
1	1	1	1	1
2	1	2	2	2
3	1	3	3	3
4	2	1	2	3
5	2	2	3	1
6	2	3	1	2
7	3	1	3	2
8	3	2	1	3
9	3	3	2	1

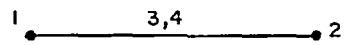

Figure 5 Linear graph of L9 table

orthogonal array specifies the number of trials to be carried out and also the combination of the levels of the various factors (treatment combination) for each run. Each column of the orthogonal array is either allocated to a factor or an interaction between the factors and fixes its level for each trial. An orthogonal array is associated with a set of linear graphs. A linear graph consists of a set of nodes and a set of lines each of which join a certain pair of nodes. All the nodes and lines are numbered. The node number denotes the column number of the array which is to be assigned to a factor while the line number denotes the column of the array which is to be assigned to the interaction effect of the factors associated with the nodes being joined. The orthogonal arrays, and their respective linear graphs for the experiments where each factor has two levels (1 and 2), are available in References 13, 15. *Table 3* and *Figure 5*, respectively, show an orthogonal array and the associated linear graph used in the present study. This array is known as L9 array and can be made use of for designing 3-level experiments.

By using an orthogonal array and its linear graph, one can estimate the effect of the factors and their interactions towards the variation of response in terms of a quantity called the contribution ratio (CR), as explained in the section for results and discussions. This method is also known as Taguchi's method since it was first proposed by G. Taguchi[15].

RESULTS AND DISCUSSION

In the first set of parametric studies the effect of change in the percentage flow rate through the swirler, the swirl number, the swirler geometry and primary injection velocity on the characteristics of the recirculation zone is investigated numerically. The change in the swirler geometry is achieved by a change of the diameter of the hub, whereas the change in the primary injection velocity is effected by a change in the diameter of the injection hole.

The three levels for each of the parameters are chosen as shown in *Table 4*. During the course of trials, only the flow rate through the swirler is varied, while the flow through the primary and dilution holes is maintained constant. The bulk Reynolds number is of the order of 6×10^4 throughout the course of trials. The change in the hub diameter will tend to change the swirl

Table 4 Factors considered

Factors		Level 1	2	3
Percentage flow through swirler	(A)	10	20	25
Swirl number	(B)	0.50	0.75	1.0
Hub diameter in mm	(C)	10	20	25
Primary hole diameter in mm	(D)	7.5	10.0	12.5

Table 5 Experimental layout and responses

Run no.	Factors A	B	C	D	Responses R	L (mm)	T (mm)
1	1	1	1	1	0.70	50.22	22.34
2	1	2	2	2	0.55	51.52	21.89
3	1	3	3	3	0.40	52.91	21.77
4	2	1	2	3	0.26	53.50	20.29
5	2	2	3	1	0.51	51.02	22.30
6	2	3	1	2	0.37	52.70	21.73
7	3	1	3	2	0.29	54.80	20.11
8	3	2	1	3	0.20	55.94	22.11
9	3	3	2	1	0.41	58.10	22.62

number for a constant vane angle. Hence, to maintain the swirl number as per requirement, the vane angle is assumed to be adjusted. Our current aim is to quantify the effects of changing the above parameters on the recirculation zone characteristics. We choose to estimate only the main effects of the factors and hence following Taguchi's method, described in detail in References 13, 15, we allocate the columns 3 and 4 of the orthogonal array, shown in *Table 3*, to the factors C and D, i.e. hub diameter and primary hole diameter, respectively. The trials are then carried out as per the layout shown in *Table 5*. The responses characterizing the recirculation zone, i.e. R, L, and T, for each run are also indicated.

From *Table 5* it is evident that the variation of L and T during the course of trials is not significant. Hence the detailed study is confined to that of variation of recirculation ratio R. The contribution ratios (CR) of the factors mentioned in *Table 4* towards the variation of R is calculated as follows:

(i) Average response (AR)

$$\mathrm{AR} = G/N$$

where
G is the grant total of all responses and
N is the number of responses.

(ii) Total sum of squares (TSS)

$$\mathrm{TSS} = \sum_{i=1}^{N} (x_i - \mathrm{AR})^2$$

where x_i denotes the individual response.

Table 6 Contribution ratios of various factors towards variation of R

Factors		Contribution ratio (%)
Flow through the swirler	(A)	55.5
Swirl number	(B)	0.1
Hub diameter	(C)	0.2
Primary hole diameter	(D)	44.2

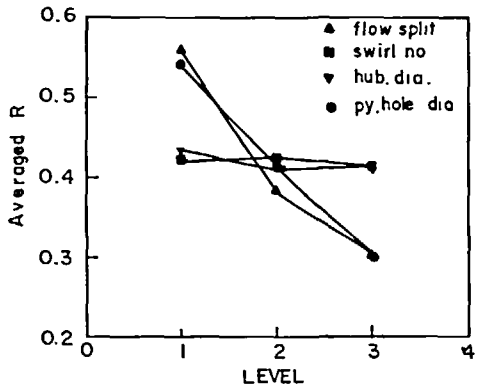

Figure 6 Effect of various factors on R

(iii) Sum of squares due to each factor (SS)
For a factor A:

$$SS_A = SS_{A,1} + SS_{A,2} + SS_{A,3}$$

where
$SS_{A,1} = n_{A,1}x$ (mean of all responses with A at level 1 − AR)^2
$SS_{A,2} = n_{A,2}x$ (mean of all responses with A at level 2 − AR)^2
$SS_{A,3} = n_{A,3}x$ (mean of all responses with A at level 3 − AR)^2
where $n_{A,1}$, $n_{A,2}$ and $n_{A,3}$ denote total number of responses with A as level 1, 2 and 3, respectively.

Similarly calculate SS_B, SS_C and SS_D

$$SS_{residuals} = TSS - (\text{sum of SS of all the main factors and interactions})$$

$SS_{residuals}$ will include the effects of all the remaining possible interactions among A, B, C and D.

(iv) Contribution ratio

$$CR = 100 \times (SS/TSS)$$

Table 6 shows the calculated contribution ratios for various factors. Therefore, the percentage of total flow through the swirler has a maximum effect on R followed by the effect of the primary hole diameter which determines the velocity of the jet for a given flow rate. In comparison to these factors, the swirl number and the swirler geometry represented by hub diameter have a negligible effect on R. These facts are represented in *Figure 6*. It shows the plot of averaged R for each factor with respect to the level of the factor. For instance the mean value of R for factor

A (i.e. the flow split) at Level 1 is the average of values of *R* obtained from the trials where this factor is at Level 1, irrespective of the levels of the other factors.

The averaged *R* shows a steep decrease from about 0.55 to 0.3 when the level of the flow split changes from 1 to 3 (i.e. when the percentage flow through the swirler is changed from 10% to 25%). The same trend is observed for a change in the level of primary hole diameter from Level 1 to Level 3 (i.e. from 7.5 mm dia. to 12.5 mm dia.). An almost horizontal line for both swirl number and hub diameter illustrates their negligible role in determining *R* when compared to that of flow splits and primary hole diameter.

Having gauged the general trends, we now study in detail the effect of various parameters on the velocity profiles. Run number 6 of *Table 5* which has the treatment combination 2312, i.e. swirler flow rate at Level 2, swirl number at Level 3, hub diameter at Level 1 and primary hole diameter at Level 2, is chosen as the base case. Trials are now carried out by changing the level of only one factor at a time. The results are summarized in *Figure 7*. The same trends for *R* is observed as in the case of averaged *R* (*Figure 6*) for all the factors except for the variation of the hub diameter. This indicates the interaction effect of the hub diameter with other factors.

The effects of flow splits, swirl number, hub diameter and primary hole diameter on the velocity profiles at the station where *R* is calculated are now discussed.

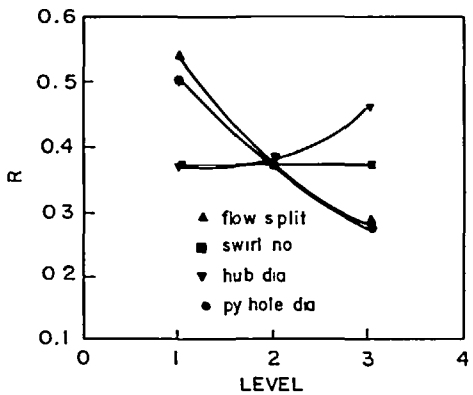

Figure 7 Variation of *R* with levels for base case 2312

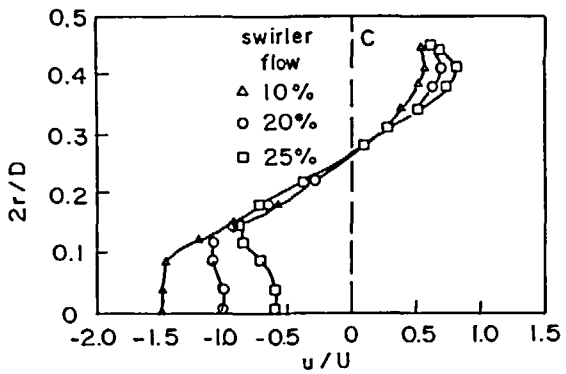

Figure 8 Effect of flow split on axial velocity

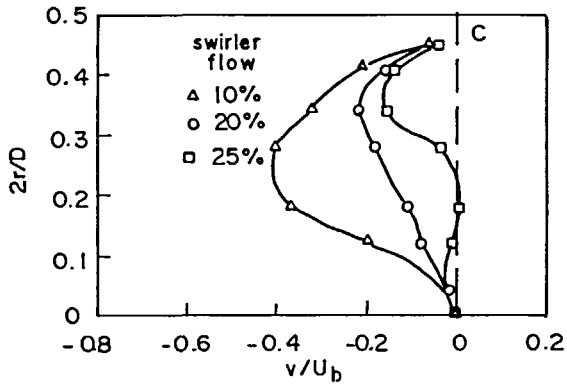

Figure 9 Effect of flow split on radial velocity

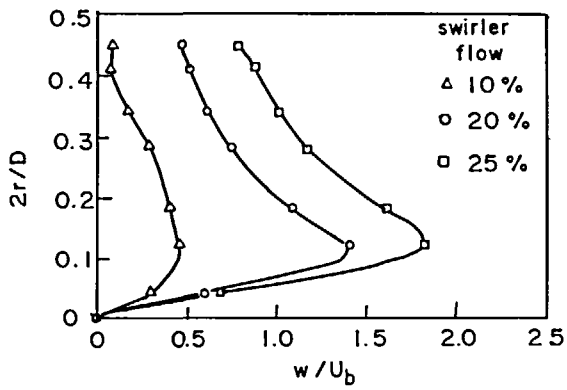

Figure 10 Effect of flow split on azimuthal velocity

(i) *Effect of flow split*

Figure 8 shows that an increase of swirler flow from 10% to 25% causes 50% reduction of maximum negative axial velocity. This corresponds to a decrease in R from 0.54 to 0.28. Weakening of the jet penetration, i.e. reduction in the negative radial velocity (as per convention velocity towards the axis is given negative sign) with increase in swirler flow rate, is observed in *Figure 9*. For a 25% swirler flow rate a central core, with no radial velocity, is formed. This core extends up to 50% of the total radius. Hence the jets do not impinge. *Figure 10* shows that the azimuthal (swirl) velocity increases with swirler flow rate. Increase in swirler flow rate also causes a shift in the point of maxima away from the axis of the combustor.

(ii) *Effect of swirl number*

It is evident, from *Figure 11*, that an increase in swirl number from 0.1 to 1.0 causes a marginal reduction in the maximum recirculation velocity. However R remains constant at 0.37 for this range. *Figure 12* shows that the negative radial velocity shifts towards zero with an increase in swirl number. However, the depth of penetration is not affected as the jets still impinge at the axis. *Figure 13* shows that, with the increase in swirl number, the azimuthal velocity also increases but without any shift in the point of maxima.

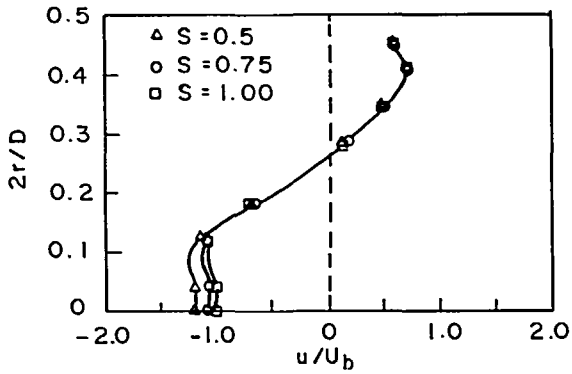

Figure 11 Effect of swirl no. on axial velocity

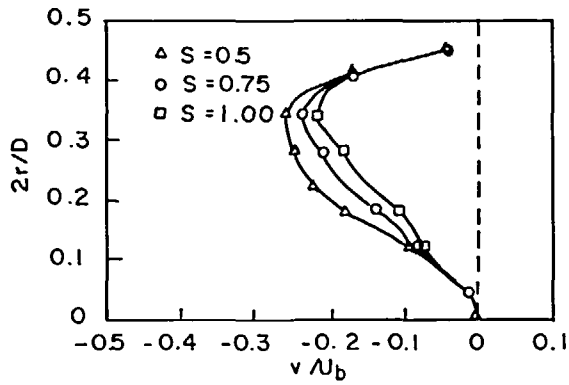

Figure 12 Effect of swirl no. on radial velocity

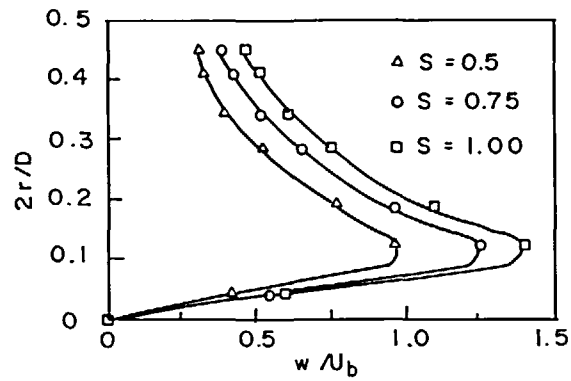

Figure 13 Effect of swirl no. on azimuthal velocity

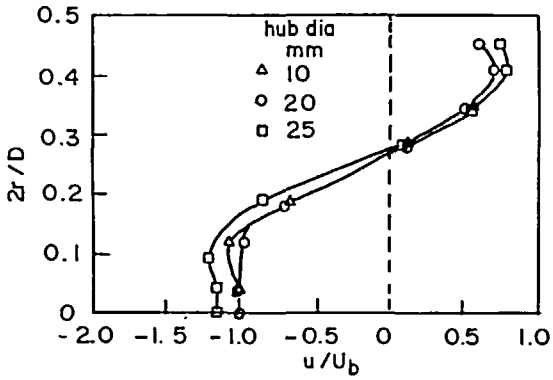

Figure 14 Effect of hub diameter on axial velocity

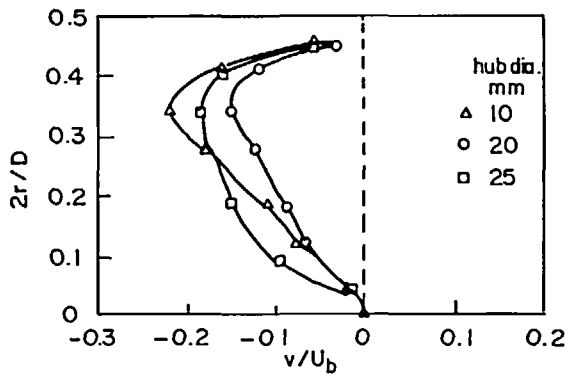

Figure 15 Effect of hub diameter on radial velocity

(iii) *Effect of hub diameter*

No definite trends could be discerned for variation of axial velocity from *Figure 14*. While there is no change in maximum recirculation velocity for an increase in hub diameter from 10 to 20 mm, there is a sudden increase of 25% when the hub diameter is further increased to 25 mm. A corresponding increase in R is from 0.38 to 0.46. This shows the interaction effect of the hub diameter with other factors. The interaction effect is also evident in the radial velocity profiles in *Figure 15*. We find that for an increase in hub diameter from 10 mm to 20 mm there is a decrease in negative radial velocity but with a further increase of hub diameter to 25 mm the negative radial velocity increases. *Figure 16* shows that the swirl velocities are nearly the same for all hub diameters to a distance of about 25% of the combustor radius from the axis. Farther away higher values of swirl velocities are found for larger hub diameters.

(iv) *Effect of primary hole diameter*

The increase in diameter of the primary holes result in a decrease in the jet velocities for a given flow rate resulting in weaker penetration resulting in a reduction in the mass of recirculated fuel. *Figure 17* shows that an increase in primary hole diameter from 7.5 mm to 12.5 mm results in a 50% reduction in the maximum recirculation velocity. The corresponding decrease in R is from 0.5 to 0.27. This increase in diameter also weakens the jet penetration considerably as

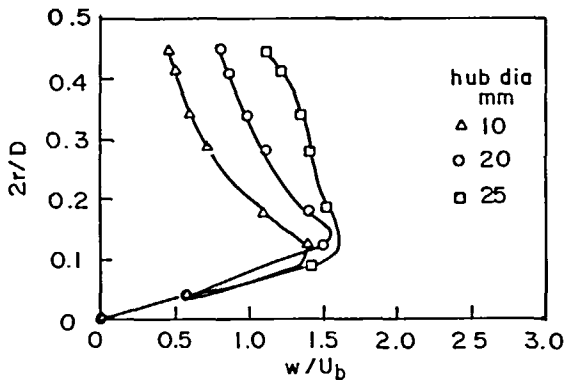

Figure 16 Effect of hub diameter on azimuthal velocity

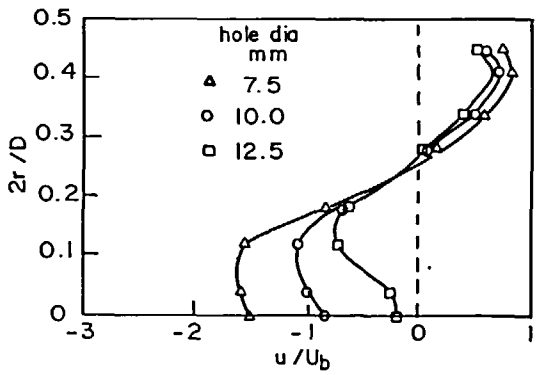

Figure 17 Effect of primary hole diameter on axial velocity

evident from *Figure 18* which shows a positive radial velocity (i.e. upward motion of the fluid) for a hole diameter of 12.5 mm at a distance of 50% of total radius from the hole itself. The swirl velocity reduces with an increase in the hole diameter near the axis but increases from the distance of about 25% of the total radius away from the axis as shown in *Figure 19*.

The previous set of parametric tests indicate that the effect of primary jets heavily dominates the effect of swirl number in determining the mass of fluid recirculated. This is indicated by a contribution ratio of about 44% for primary hole diameter towards the variation of R as against negligible contribution ratio (0.1%) of the swirl number. It is also evident from *Figure 11* where for a given swirler flow rate of 20% primary hole diameter of 10 mm and a hub diameter of 10 mm the variation of swirl number hardly has any effect on negative axial velocity as a result of which R remains constant. Also the change in the length of the recirculation zone during the course of the L9 experiment as per *Table 5* is not much.

At this stage we briefly discuss the main results obtained from an earlier numerical study conducted by the authors[11] in absence of primary injection holes for the same combustor geometry. A full factorial experiment was conducted using an L9 array for a given swirler flow rate for three levels of swirl numbers (S) viz., 0.5, 0.75 and 1.0 and three levels of hub diameter, viz. 10 mm, 20 mm and 25 mm. *Table 7* shows the layout of the experiment and also the values of R, L and T corresponding to each run. The contribution ratios of the individual effects and interaction effects were calculated. These values are shown in *Table 8*. From this table it is clear

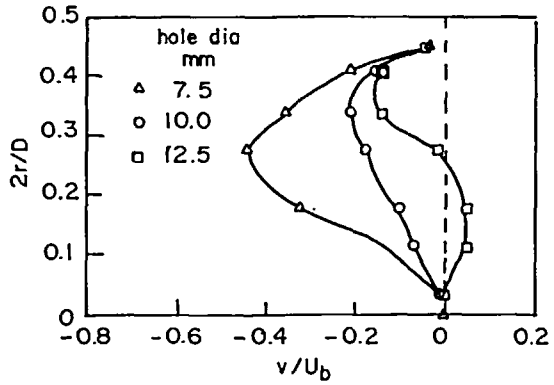

Figure 18 Effect of primary hole diameter on radial velocity

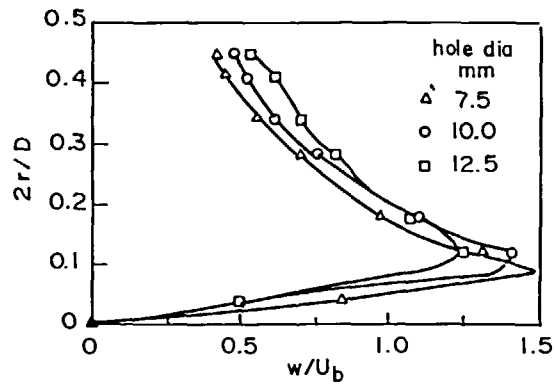

Figure 19 Effect of primary hole diameter on azimuthal velocity

Table 7 Swirler effects on recirculation zone in the absence of primary jets

Run no.	Factors B (Swirl no.)	Factors C (Hub dia.)	Interaction columns 3	Interaction columns 4	Responses R	Responses L (mm)	Responses T (mm)
1	1	1	1	1	0.20	91	14.89
2	1	2	2	2	0.18	94	12.21
3	1	3	3	3	0.26	88	12.38
4	2	1	2	3	0.42	88	19.66
5	2	2	3	1	0.53	85	18.59
6	2	3	1	2	0.52	85	17.30
7	3	1	3	2	0.53	100	20.63
8	3	2	1	3	0.89	83	21.32
9	3	3	2	1	0.94	82	22.13

Note: Total flow rate = 3.5 kg/s

Table 8 Contribution ratios of swirler effects in the absence of primary jets

	Contribution ratio (%)		
Factor	*R*	*L*	*T*
B (Swirl no.)	81.7	14.1	92.5
C (Hub dia.)	10.0	38.2	2.1
B X C (Interaction)	8.3	47.8	5.4

Table 9 Effect of decreasing the primary jet strength

$\frac{\dot{m}_{sw}}{\dot{m}_{tot}}$ (%)	$\frac{\dot{m}_{sw}}{\dot{m}_{pr}}$ (%)	$\frac{\dot{m}_{sw}}{\dot{m}_{pr}}$	*R*	*L* (mm)	*T* (mm)
10	40	0.25	0.56	51.5	22.7
20	30	0.67	0.37	52.3	21.7
25	25	1.00	0.24	71.5	22.5
30	20	1.50	0.20	94.2	21.4
35	15	2.33	0.28	103.2	20.7
40	10	4.00	0.36	103.1	20.6
45	5	9.00	0.45	102.8	20.8
50	0	∞	0.53	100.8	20.9

Note: (i) $\dot{m}_{tot} = 3.5$ kg/s; $\dot{m}_{sec} = 1.75$ kg/s; (ii) primary hole diameter = 10 mm; hub diameter = 10 mm

that the recirculation ratio *R* and the thickness of the recirculation zone *T* is determined mainly by the swirl number the contribution of which is more than 80% in the case of former and more than 90% in the case of the latter. Higher swirl numbers tend to increase *R* and *T*, but its individual effect on the length of the recirculation zone is only 14%. It is the interaction of swirl number with hub diameter which plays a more important role by contributing about 48% towards the variation of length of recirculation zone. The individual effect of hub diameter on the length of recirculation zone is also quite significant (contribution ratio of 38%). Another interesting feature to be noted is that while in the presence of primary jets the length of the recirculation zone is around 50 mm to 55 mm, *Table 5*, it is of the order 80 mm to 100 mm, *Table 7*, in their absence. This leads to the inference that the primary jets have a restrictive effect on the length of the recirculation zone.

We therefore see that the effects of the swirler on the characteristics of the recirculation zone are negligible compared to that of primary jets but considerable when the primary jets are absent. This indicates a possibility of the presence of a critical point at which the swirler effects overcome the effects of primary jets on the recirculation zone structure. The knowledge of this critical point may be of significant use to combustor designers. We now proceed to find out the critical point for the combustor, by decreasing the flow through the primary holes gradually so that the ratio of mass flow rate through the swirler to that through the primary hole increases correspondingly. The overall flow rate is maintained constant throughout. The results obtained are shown in *Table 9*.

Variation of *R* with respect to $\dot{m}_{sw}/\dot{m}_{pr}$ is shown in *Figure 20*. With the increase of $\dot{m}_{sw}/\dot{m}_{pr}$, *R* decreases from 0.56 to 0.20 until $\dot{m}_{sw}/\dot{m}_{pr}$ reaches a value of 1.5. This reduction in *R* is due to reduction in primary jet velocity corresponding to a decrease of flow through the primary

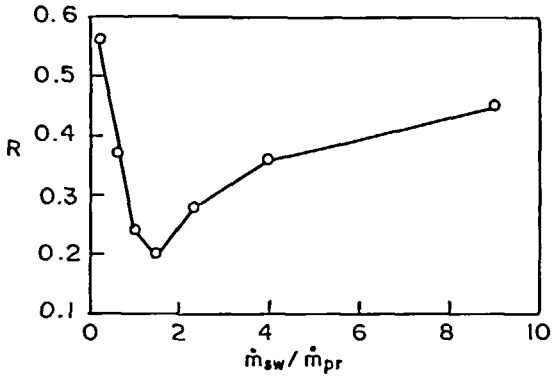

Figure 20 Variation of R with $\dot{m}_{sw}/\dot{m}_{pr}$

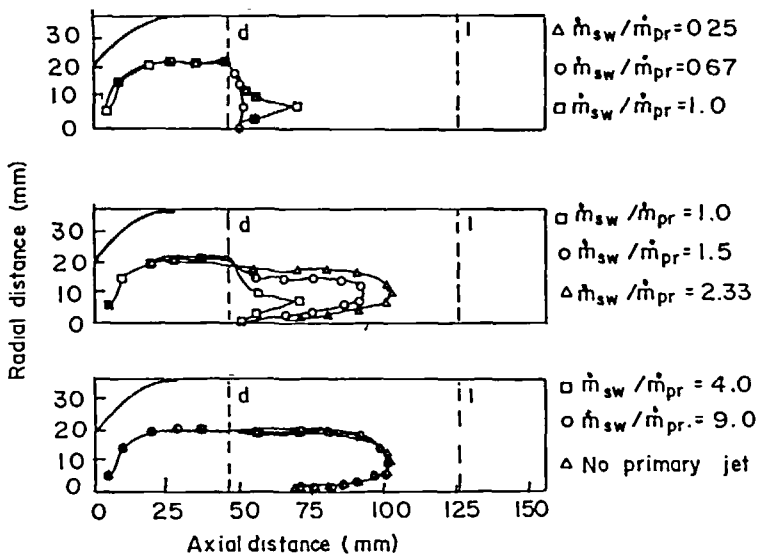

Figure 21 Effect of $\dot{m}_{sw}/\dot{m}_{pr}$ on recirculation zone

holes. As a consequence the penetration of jets has weakened. However, with a further increase in $\dot{m}_{sw}/\dot{m}_{pr}$ there is an increase in R. Hence $\dot{m}_{sw}/\dot{m}_{pr} = 1.5$ is the critical point. This corresponds to 30% of the total flow through the swirler and 20% through the primary holes. The increase in R after the critical point is due to the swirler taking over the role, from the primary jets, in providing recirculation. The R increases continuously with decrease in flow through the primary holes until the limiting case of absence of primary jets is reached. R at this point is 0.53, *Table 9*, which is almost the same as that for $\dot{m}_{sw}/\dot{m}_{pr} = 0.25$.

Figure 21 shows the variation of recirculation zone area with increase in $\dot{m}_{sw}/\dot{m}_{pr}$. The dashed line indicates the position of primary and dilution holes. For $\dot{m}_{sw}/\dot{m}_{pr} = 0.25$ and 0.67 there is no change in the area of the recirculation zone. As this ratio approaches the value 1.0 the recirculation zone starts increasing. This trend is continued until $\dot{m}_{sw}/\dot{m}_{pr} = 2.33$ after which the recirculation zone length remains unchanged until the limiting case of absence of primary jets is reached. We see that, by completely diverting the flow through the primary holes to the

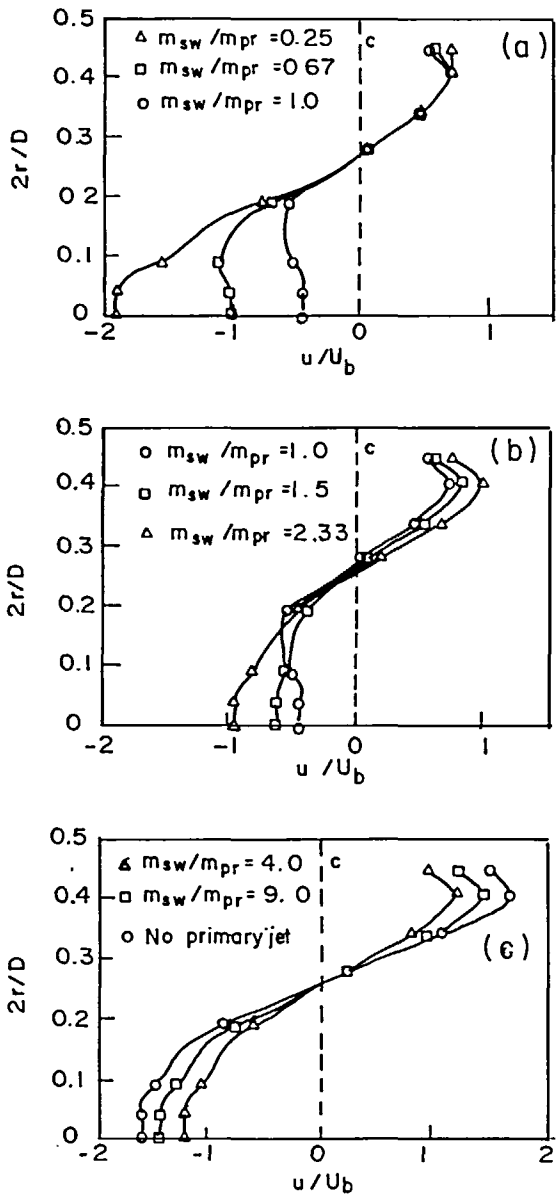

Figure 22 Effect of $\dot{m}_{sw}/\dot{m}_{pr}$ on axial velocity

swirler, it has been possible to increase the length of recirculation zone almost double, from about 51 mm to about 100 mm. The maximum thickness of the recirculation zone however remains constant for all the flow rates.

Figures 22–24 show the axial, radial and azimuthal velocity profiles at station 'c' corresponding to the change in flow rate through the primary holes and swirler. *Figure 22* shows that there is a decrease in maximum recirculation velocity of 75% with an increase in $\dot{m}_{sw}/\dot{m}_{pr}$ from 0.25 to 1.0. After this point, the maximum recirculation velocity increases until it reaches about three

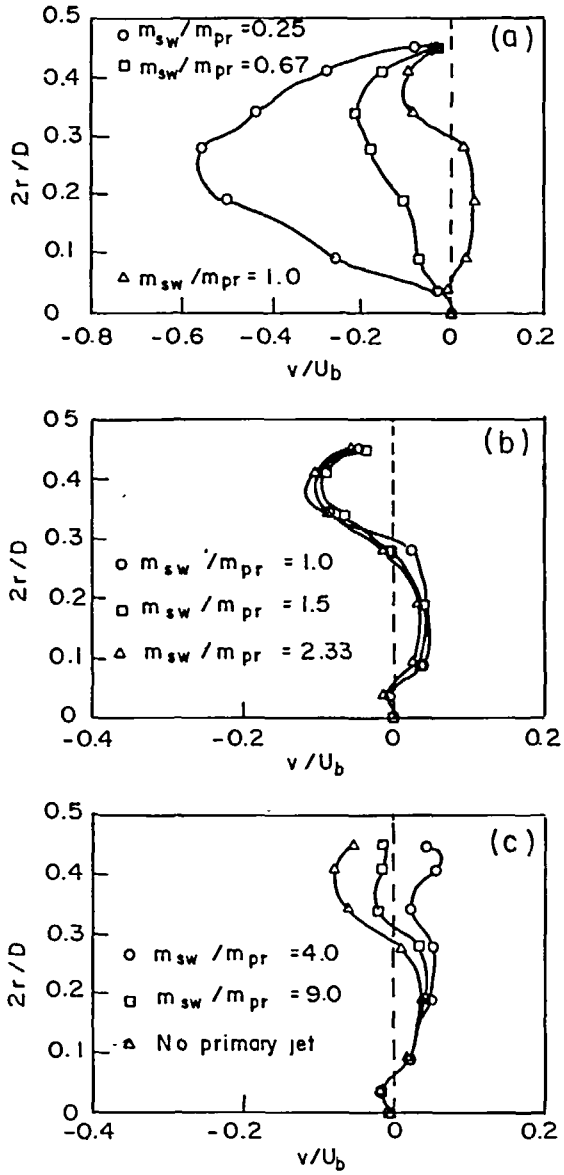

Figure 23 Effect of $\dot{m}_{sw}/\dot{m}_{pr}$ on radial velocity

times the value, about 75% of the original value, of that at $\dot{m}_{sw}/\dot{m}_{pr} = 1.0$ for the limiting case of absence of primary jets.

An increase in $\dot{m}_{sw}/\dot{m}_{pr}$ tends to reduce the negative radial velocity due to weakening of the primary jets. This is shown in *Figure 23*. At $\dot{m}_{sw}/\dot{m}_{pr} = 1.0$ about 60% of the combustor radius has a positive radial velocity and, in the complete absence of primary jets, positive radial velocities prevail almost throughout the cross-section at this station. *Figure 24* shows that for the range $\dot{m}_{sw}/\dot{m}_{pr} = 0.25$ to 1.0 the swirl velocity increases. The point of maximum progressively shifts away from the centre. For the range $\dot{m}_{sw}/\dot{m}_{pr} = 1.0$ to 2.33 the swirl velocity increases up to a

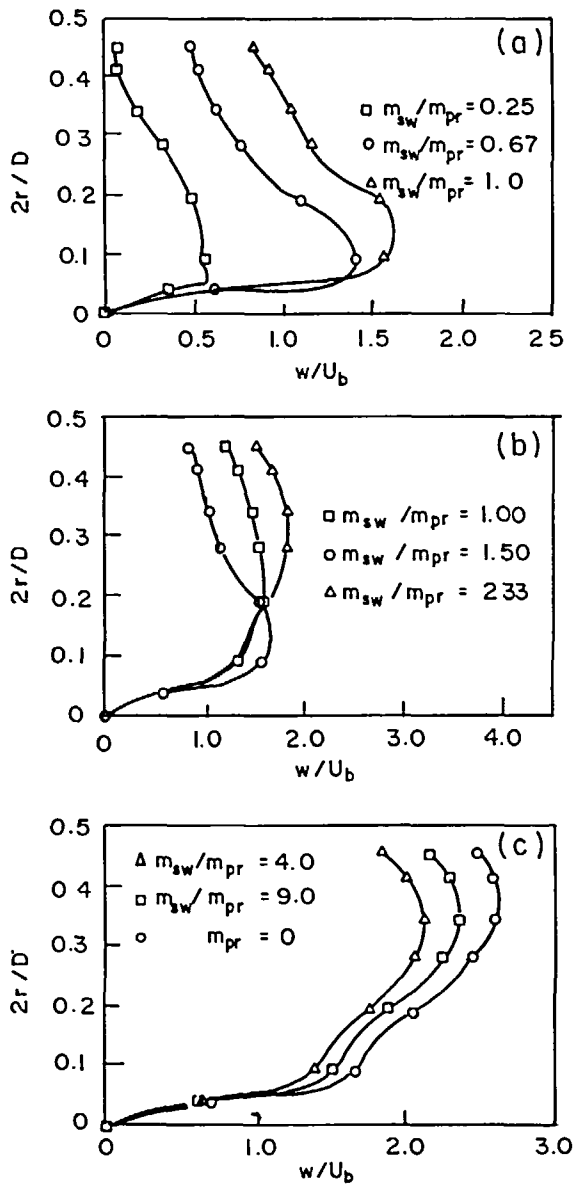

Figure 24 Effect of $\dot{m}_{sw}/\dot{m}_{pr}$ on azimuthal velocity

distance of 40% of the combustor radius from the axis and decreases beyond this point. For the range $\dot{m}_{sw}/\dot{m}_{pr} = 2.33$ and above, the swirl velocity increases progressively. The point of maximum is now shifted to a distance of about 60% of the combustor radius away from the axis.

CONCLUSIONS

General conclusions that can be drawn from these numerical parametric studies for isothermal

flows are as follows:

(i) Flow rate through the swirler and primary jets almost entirely determine the recirculation zone characteristics. Lower flow rates and higher jet velocities yield better recirculation.
(ii) The effect of the primary jet is to restrict the length of the recirculation zone.
(iii) Swirler effects take over the role of determining the recirculation zone characteristics only if the velocity of the primary jets is low.
(iv) A longer recirculation zone results in the absence of primary jets. Its thickness is now determined by the swirl number – thicker for higher swirl numbers. In absence of primary jets the recirculation ratio R increases with swirl number.

An optimum recirculation zone is essential for ensuring proper combustion in a gas turbine combustor. From this study it is recommended that for ensuring a good recirculation in terms of mass of fluid, i.e. R, the velocity of the jets through the primary injection holes should be increased and the inlet flow rate through the swirler may be kept at a minimum value dictated by practical considerations. Also, it is suggested that less attention can be given to the swirler design modifications in view of its negligible effect in comparison to the inlet flow rate and the primary jet velocity. Orthogonal array experiments will provide fairly representative values, from a set of all responses that could have been obtained, if all possible combinations of the factors have been tested. Hence, based on the responses obtained in this study, *Table 5*, in order to get a maximum recirculation ratio R, all the factors should be kept at Level 1, see *Table 5*, Run 1, i.e. 10% flow through the swirler, a primary hole diameter of 7.5 mm, swirl number of 0.5 and the hub diameter of 10 mm. If a long recirculation zone is desired then from *Table 5* we find that this can be achieved by using the treatment combination 3321 of Run 9, i.e. 25% swirler flow, primary hole diameter of 7.5 mm, a swirl number of 1 and a hub diameter of 20 mm. A better way to achieve a longer recirculation zone would be to shift the location of the row of primary holes downstream, since it has been shown that the length of the recirculation zone is determined by the position of the primary holes.

Several other parameters can be considered and analyzed numerically by using OAT. However, a greater number of trials may have to be performed. However, it will be still economical in terms of time and resources compared to that of physical experiments. Hence, it is hoped that such studies applying OAT to a numerical code will serve as an aid to the gas turbine combustor designer.

REFERENCES

1 Altgeld, H., Jones, W. P. and Whilhelmi, J. Velocity measurement in a confined swirl driven recirculating flow, *Experiments in Fluids*, **1**, 73–78 (1983)
2 La Rue, J. C., Samuelsen, G. S. and Seiler, E. T. Momentum and heat flux in a swirl stabilized combustor, *Proc. 20th Int. Symp. Combust.*, The Combustion Institute (1984)
3 Rhode, D. L., Lilley, D. G. and McLaughlin, D. K. Mean flow fields in axisymmetric combustor geometries with swirl, *AIAA J.*, **21**, 593–600 (1983)
4 Vu, B. T. and Gouldin, F. C. Flow measurements in a model swirl combustor, *AIAA J.*, **20**, 642–651 (1982)
5 Kahn, Z. A., McGuirk, J. J. and Whitelaw, J. H. A row of jets in a crossflow, AGARD CP308 (19??)
6 Koutmos, P. and McGuirk, J. J. Isothermal flow in a gas turbine combustor – a benchmark experimental study, *Experiments in Fluids*, **7**, 344–354 (1989)
7 Koutmos, P. and McGuirk, J. J. Investigation of swirler/dilution jet flow split on primary zone flow patterns in a water model can-type combustor, *J. of Engng. for Gas Turbines and Power*, **111**, 310–317 (1989)
8 Koutmos, P. and McGuirk, J. J. Isothermal modeling of gas turbine combustors: computational study, *J. Propulsion*, **7**, 1064–1071 (1991)
9 Patankar, S. V. and Spalding, D. B. A calculation procedure for heat, mass and momentum transfer in three dimensional parabolic flows, *Int. J. Heat Mass Transfer*, **15**, 1787–1806 (1972)
10 Sampath, S. and Ganesan, V. Numerical prediction of flow and combustion in three dimensional gas turbine combustor, *J. Inst. Energy*, **60**, 13–28 (1987)
11 Gopinath, R. and Ganesan, V. Numerical study of swirler effects on the recirculation zone of a gas turbine combustor by means of design of experiments technique, *Proc. 1st Nat. Conf. on Air Breathing Engines*, 234–239 (1992)

12 Gopinath, R. Computer modelling of three-dimensional flows in a gas turbine combustor, *PhD Thesis*, IIT Madras (1993)
13 Gopinath, R. and Ganesan, V. Orthogonal arrays – an introduction and their application in optimizing underrelaxation factors in a SIMPLE based algorithm, *Int. J. Num. Methods for Fluids*, **14**, 665–680 (1992)
14 Juran, J. M. and Grynaa, F. M. *Juran's Quality Control Handbook*, McGraw-Hill, New York, 26.1–26.81 (1988)
15 Lecture notes on the course entitled *Industrial Experimentation*, Indian Statistical Institute, Bangalore (1986)